Kondoesque origin of resistivity anisotropy in graphite

L. Craco,[1] M. S. Laad,[2] S. Leoni,[3] and A. S. de Arruda[1]
[1]*Instituto de Física, Universidade Federal de Mato Grosso, 78060-900, Cuiabá, Mato Grosso, Brazil*
[2]*Institut Laue-Langevin, 6 Rue Jules Horowitz, 38042 Grenoble Cedex, France*
[3]*Physical Chemistry, Technical University Dresden, 01062 Dresden, Germany*
(Received 10 December 2012; revised manuscript received 31 January 2013; published 3 April 2013)

Based on a careful perusal of data, we revisit the longstanding issues of transport anisotropy and incoherence-coherence crossovers in graphite. Using a realistic many-body approach, we unearth surprising but distinctive signatures of band-selective Kondoesque physics in graphite. The intricate interplay between local multiband Coulomb and *effectively* enhanced residual spin-orbit interactions comprehensively rationalizes these anomalies in terms of a manifestation of a multiband Kondo effect with a small Fermi liquid coherence scale.

DOI: 10.1103/PhysRevB.87.155109 PACS number(s): 75.20.Hr, 72.10.Fk, 74.25.F−, 75.70.Tj

I. INTRODUCTION

Graphite, the best known bulk allotrope of elemental carbon, has attracted considerable attention due to its potential applications.[1] Moreover, the discovery of fullerenes,[2] carbon nanotubes,[3] and graphene[4] have renewed this interest. On a fundamental front, large magnetoresistance,[5] magnetic-field driven metal-insulator transitions,[6] an unusual Landau level energy spectrum,[7] and the quantum Hall effect[5] constitute rather strong evidence for electronic correlations in graphite. However, in spite of incisive studies,[8,9] these unusual responses remain mostly ill-understood issues of fundamental importance.

Interestingly, graphite also shows related and poorly understood anisotropy in magnetic susceptibility[10] and electrical transport[11] responses. Specifically, resistivity data[5,6,11–14] in graphite is intriguing. In single crystals, a "huge" resistivity anisotropy, with the ratio $[\rho_c(T)/\rho_a(T)] \simeq 100$ below 200 K,[11] is seen. In purely band structure considerations, transport should be semimetallic[15,16] due to the dominant role of p_z bands[17] near the Fermi energy E_F. In reality, transport and spectroscopic data in graphite pose a rather serious problem for the local-density approximation (LDA), actually showing a very intriguing trend: The in-plane resistivity $[\rho_a(T)]$ is that of a "good" normal metal, showing T^2 Fermi liquid (FL) behavior, albeit below an extremely low-energy scale of 5 K,[12] followed by a quasilinear T dependence and saturation at higher temperatures. In stark contrast, the out-of-plane resistivity decreases with increasing T and shows insulating-T dependence above a characteristic but rather low (material specific) temperature T^*, which is 175 K for single crystals and about 40–50 K for highly oriented pyrolitic graphite (HOPG). Importantly, true FL-like behavior is only recovered below 5 K. These are strong indicators for (i) drastically renormalized FL behavior as evidenced in $\rho_{ab}(T)$ and (ii) unconventional out-of-plane dynamics. Interestingly, (ii) is closer to what is found in d-band oxides such as Sr_2RuO_4,[18] strongly suggesting the relevance of hitherto scantily studied anisotropic interactions. This anisotropy is even more enhanced in thin films and flakes of graphite, and its microscopic understanding is thus important for devising strategies for device manipulation.[14] Concomitantly, angle-resolved photoemission (ARPES) data show a very narrow low-energy feature close to E_F in graphite.[19–22] Significantly, this sharp electronic quasiparticlelike feature is neither expected nor predicted by bulk band structure calculations.[15–17] In spite of a number of scenarios[19–22] proposed to rationalize this, its origin remains enigmatic. Finally, electron-spin resonance (ESR)[23] data show that transport anomalies are strikingly correlated with the T dependence of ESR linewidths and g factors,[23] and, in fact, that the onset of true FL metallicity is intimately linked to suppression of fluctuations of an "internal" magnetic field associated with spin-orbit coupling (SOC). Adopting a broader perspective, these spectral and transport features must be correlated with ESR data: Thus, could it be that the origin of the narrow feature in ARPES has an intimate connection with the anisotropic emergence of FL behavior *and* suppression of longitudinal (ESR) field fluctuations below a (anisotropically renormalized) very low-energy scale? This striking but ill-understood (and unappreciated) correlation should thus hold the key to a much deeper understanding of graphite.

Here, we address the microscopic origin of these surprising behaviors in graphite. Our main result is that, in addition to the competition between itinerance and local Hubbard interactions, a surprising element induced by SOC plays a key role in the rationalization of the above features. We use LDA plus dynamical mean-field theory (LDA + DMFT) as a working tool because it is particularly suited for many correlated materials,[24] and has also been used recently in the context of Kondo and Mott physics in topological insulators.[25] On a qualitative physical level, realistic Coulomb interactions in the peculiar band-selective (coexistent semimetallic and band insulating) density of states (DOS) of graphite (a feature already evident in LDA—see below) are expected to lead to the emergence of different features, an expectation fully borne out below by explicit computations. Moreover, the internal consistency with ESR data,[23] along with good semiquantitative accord with (AR)PES[19] and the transport[12,13] data above, cements this basic view, unveiling the fundamental roles of sizable electronic correlations and the (hitherto scantily studied) SOC in graphite.

II. THEORY AND DISCUSSION

The crystal structure ($P6_3/mmc$ space group) of graphite is a Bernal stacking of graphene layers.[16] Weak interactions between planes convert the zero-gap Dirac spectrum of

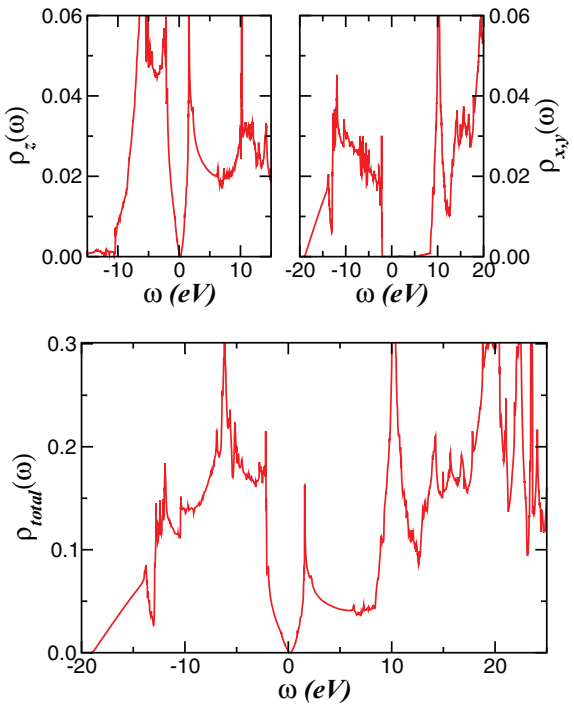

FIG. 1. (Color online) LDA orbital-resolved (upper panels) and total (lower panel) density of states (DOS) of graphite. Notice the Dirac-like DOS near the Fermi energy ($E_F = \omega = 0$) in LDA.

graphene[26] to a semimetal with a small number of p_z valence band states crossing E_F, as in Fig. 1. We performed LDA calculations for the real crystal structure using the linear muffin-tin orbital (LMTO)[27] scheme in the atomic sphere approximation. Self-consistency is reached by performing calculations with 1326 irreducible $\mathbf{k}$ points on a $32 \times 32 \times 24$ $\mathbf{k}$ mesh for the Brillouin-zone integration. The radii of the atomic spheres were chosen as $r = 1.520$ a.u. in order to minimize their overlap. The corresponding orbital-resolved and total LDA DOS is shown in Fig. 1, in good agreement with previous studies,[15,16,28] showing broad valence and conduction bands with a band gap in the $p_{x,y}$ sector and Dirac-type (V shaped) p_z bands near E_F. This is our realistic one-electron input for incorporation of many-body effects.

Bare Coulomb interaction parameters for graphite are on-site $U_{00} = 17.5$ eV and nearest-neighbor $U_{01} = 8.6$ eV.[29] We choose both bare and renormalized values for comparison. Owing to the semimetallic LDA DOS, one would naively expect the Hubbard U to be rather poorly screened (albeit differently for single crystal and HOPG) at low energy in graphite,[15,16,28] as compared to typical good metals.

The one-electron (LDA) Hamiltonian for graphite is

$$H_0 = \sum_{\mathbf{k},a,\sigma} \epsilon_a(\mathbf{k}) c^\dagger_{\mathbf{k},a,\sigma} c_{\mathbf{k},a,\sigma} + \sum_{i,a,\sigma} (E_a - \mu) n_{i,a,\sigma}, \qquad (1)$$

where $a = x,y,z$ label the diagonalized p bands, μ is the chemical potential, and the E_a are on-site orbital energies in the real structure of graphite. Motivated by the discrepancy between LDA and transport and spectroscopic data as above, we posit that multiband Coulomb and small SOC terms are necessary to bridge this inconsistency. Recourse to small SOC may sound strange at first. However, ESR studies[23] show a large anisotropic increase (almost a factor of 3 for $H \perp c$ and 10 for $H||c$) in field shifts between 5 and 300 K, and, in fact, it has been long known that "a reliable theory for the g factor in graphite remains to be developed."[30] This points to the importance of an enhanced *effective* SOC. (A related relevant point is that there are no estimates of the SOC in graphite in a framework including interaction effects, and extant estimates rely on free-electron values.) Generically, we expect correlations to lead to an *effective* enhancement of SOC.[31] In a multiband view such as the one we adopt, J_H can cause an *effective* enhancement of SOC: This effect cannot be captured by an effective one-band model. With these arguments (the Appendix gives further discussion on the physical mechanism which leads to an enhancement of the bare SOC in graphite), the interaction terms read

$$H_{\rm int} = U \sum_{i,a} n_{i,a,\uparrow} n_{i,a,\downarrow} + U' \sum_{i,a\neq b} n_{i,a} n_{i,b} + V \sum_{i,a} (c^\dagger_{i,a,\uparrow} c_{i,a,\downarrow} + \text{H.c.}). \qquad (2)$$

Here, $U' \equiv U - 2J_H$, with U' being the interorbital Coulomb repulsion. J_H and V are, respectively, the Hund's rule and the local SO interaction. The SOC now acts as a transverse magnetic field[32] and locally mixes the p_a states of graphite. Our form for the SOC exploits the "rapid modulation limit" of Huber *et al.*[23] and is an approximation: Thus, our work is a realistic model, rather than a fully first-principles description of graphite. Concretely, we start with the bare tiny value of $V \simeq O(1\text{–}5)$ K, supplemented by the bare Hartree-Fock (HF) value $-J_H \langle b^\dagger_{i\downarrow} b_{i\uparrow} \rangle$ which arises from the Hund's term (see the Appendix; this decoupling can now be done since such a spin-flip term already exists in the bare SOC part of H in the Huber approximation). This effective SOC which becomes effectively negative will, of course, be self-consistently renormalized by local dynamical correlations beyond static HF in multiorbital (MO)-DMFT. However, we find that keeping purely local interactions[25,33] still does not improve the picture (see below): In-plane "coherent" metallicity[11,12] is not reached by correlations presented in $H_{\rm int}$, because the chemical potential μ self-consistently remains in the band gap (not shown). We have thus explored the known role of the nearest-neighbor Coulomb interaction[29,34] between electrons in the p_a bands as a way to cure this problem. This term reads

$$H^1_{\rm int} = \frac{U_1}{2} \sum_{\langle ij\rangle,a,\sigma,\sigma'} n_{i,a,\sigma} n_{j,a,\sigma'}. \qquad (3)$$

Here, $\langle ij \rangle$ denotes nearest neighbors, $a = (x,y,z)$, and $\sigma = \uparrow,\downarrow$. We treat our *extended* multiorbital (MO) Hubbard model plus local-SOC, $\bar{H} = H_0 + H_{\rm int} + H^1_{\rm int}$, using LDA + DMFT.[24] As in earlier work,[36] we decouple $H^1_{\rm int}$ in the Hartree approximation, which is exact as $d \to \infty$. On the other hand, dynamical effects arising from local interactions (U,U',J_H,V) to the self-energy $\Sigma_a(\omega)$ are only reliably estimable via DMFT.[24] We use the MO iterated-perturbation theory (MO-IPT)[37] as an impurity solver for DMFT. The detailed formulation of MO-IPT for correlated electron systems has already been developed[37] and used in Ref. 25, so we do not repeat the equations here.

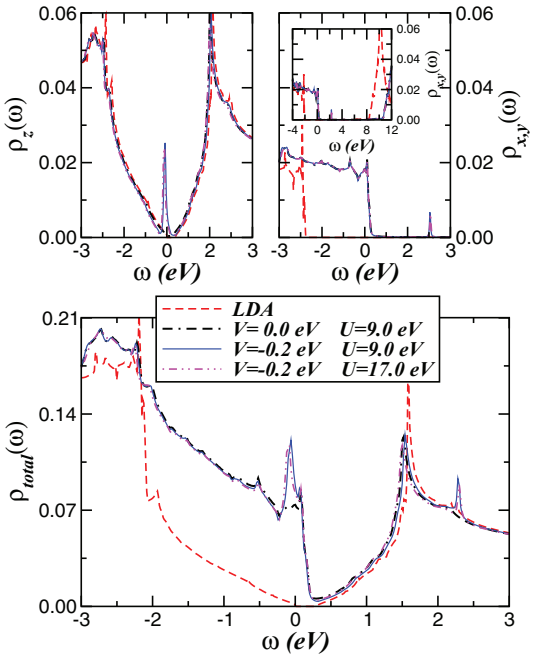

FIG. 2. (Color online) LDA (dashed) and LDA + DMFT orbital-resolved (upper panels) and total (lower panel) density of states (DOS) of graphite, the latter with fixed $J_H = 0.4$ eV and $U_1 = 5.9$ eV. Notice the tiny peak, induced as a multiband electronic reconstruction, at E_F in DMFT.

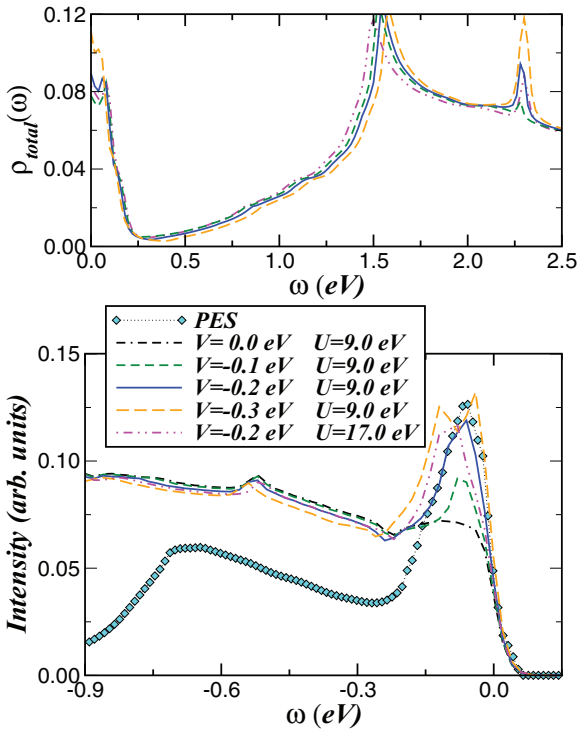

FIG. 3. (Color online) Comparison between the LDA + DMFT DOS and photoemission (PES) data for a graphite single crystal (Ref. 19): The PES curve is shifted upward in energy by 0.06 eV to coincide with theory at low energies. As seen, the main low-energy peak at −0.06 eV is accurately resolved within LDA + DMFT. The top panel shows the combined effect of Hubbard and spin-orbit interactions in the conduction band of graphite. Notice the Dirac point at 0.25 eV and the evolution of the sharp peak structure at 2.3 eV. [Apparently, in inverse-photoemission spectroscopy this unoccupied electronic feature is seen at 3.5 eV above E_F (Ref. 35).]

In Fig. 2, we display our LDA + DMFT results for two values of U (with $U' \equiv U - 2J_H$) and fixed $J_H = 0.4$ eV, $U_1 = 5.9$ eV, and total band filling $n_t = 2.0$, showing the anisotropically renormalized electronic structure of graphite. E_F is adjusted to be close to the Dirac point by following the usual practice[38] where the correct band filling is respected by self-consistently adjusting the chemical potential μ and the on-site energy E_z. Several interesting features compared to LDA are manifested in Fig. 2: Correlations promote an upward shift of the valence σ band, and the E_F is now self-consistently renormalized so as to create a small number of holes ($\approx$0.01) in the p_x, p_y orbitals, bringing the Fermi level into the σ band almost without depleting the π band. This shift is a specific effect of U_1, and creates the conditions necessary to resolve the inconsistency detailed above. Inclusion of dynamic correlations due to U, U', V now generates interesting spectral-weight transfer (SWT) induced features. The most important one (Fig. 2) is the appearance of a sharp peak in the p_z spectral function at low energy. In particular, LDA + DMFT resolves a very narrow quasiparticle resonance centered at −0.06 eV, i.e., inside the p_z Dirac band dispersion, along with clear nonvanishing DOS at E_F and reconstructed spectral functions characterized by the presence of quasicoherent electronic states (due to SWT) at low energies.

The above is in good accord with low-energy PES data of graphite single crystals,[19] as shown in Fig. 3. LDA + DMFT spectra resolves the line shape of the main peak structure including its width. The relevance of the SOC is seen in that the sharp[21] low-energy peak at 0.06 eV binding energy is *not* resolved for $V = 0$. This narrow resonance thus evolves from the interplay between small SOC and local Hubbard interactions in the *renormalized* band structure, providing a Kondoesque interpretation (see below) to the low-energy feature probed in PES experiments.[19–22]

In Fig. 4, we show the orbital-resolved self-energies for the parameter values used in Fig. 3. Surprisingly, along with resistivity results found below, behavior very akin to highly anisotropic metals showing incoherence-coherence crossovers along more resistive directions as a function of T (the best MO example of which is Sr_2RuO_4)[18] is seen. Specifically, $\mathrm{Re}\Sigma_z(\omega)$ has a large negative slope with a divergence at energies close to E_F: However, it is still consistent with a correlated FL form, albeit with a very small quasiparticle weight ($Z_{\mathrm{FL}} = [1 - (d/d\omega)\mathrm{Re}\,\Sigma_z(\omega)]|^{-1}_{\omega=E_F}$). As seen in Fig. 4, $\mathrm{Im}\Sigma_z(\omega)$ simultaneously shows a sharp pole very close to E_F. Thus, the system is surprisingly close to incoherence along the c direction, and a quasicoherent response should only be obtained at low T as a consequence of an incoherent-to-coherent crossover. True correlated FL behavior should be obtained at an even lower T, consistent with the $T_{\mathrm{FL}} \simeq 5$ K below which a T^2 dependence of the resistivity is seen experimentally.

Interestingly, all this is faithfully reproduced in transport anisotropy, which in DMFT only involves using the correlated, orbital-resolved spectral functions within the Kubo

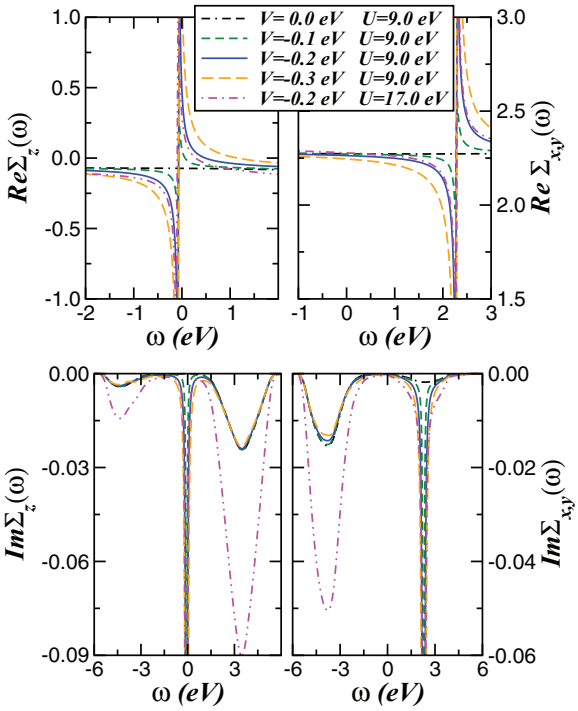

FIG. 4. (Color online) Orbital-resolved LDA + DMFT self-energies for graphite. Bottom panels: Imaginary parts, showing sharp poles very close to E_F and at 2.3 eV for the p_z and the p_x, p_y orbitals, respectively. Top panels: The corresponding real parts. These suggest that pure graphite is a drastically renormalized FL metal at very low T, but quite close to a dynamically decoupled-layer regime.

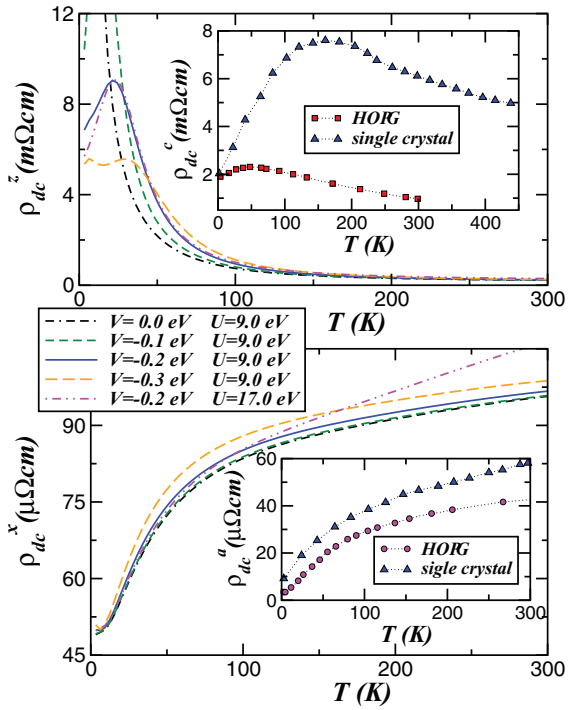

FIG. 5. (Color online) LDA + DMFT dc resistivity of graphite as a function of temperature: Very good semiquantitative agreement with HOPG data ($\rho^c_{\rm dc}$ from Ref. 13 and $\rho^a_{\rm dc}$ from Ref. 12), including details of in- and out-of-plane T dependences and crossover scales, is seen. Specifically, the insulator-metal crossover in $\rho^z_{\rm dc}$ at 21 K is in good accord with HOPG data. (Single-crystal data is taken from Ref. 11.)

formalism.[39] The dc resistivity in Fig. 5 shows orbital selectivity manifesting as directional selectivity. In the upper panel of Fig. 5, we display the c-axis resistivity of graphite. As discussed above, $\rho^z_{\rm dc}(T)$ strongly increases as $T \to 0$ for $V = 0$, consistent with the semiconducting behavior expected for interlayer transport in a system having a Dirac spectrum. Interestingly, switching on SOC leads to enhanced metallicity accompanying an insulator-metal crossover. Local spin fluctuations[32] thus promote a smooth crossover to low-energy quasicoherence by internally generating a spin-flip channel that switches on the recoil process locally: If this had not occurred, one would have an incoherent metal down to lowest T. This is our mechanism for a strong reduction of $\rho^z_{\rm dc}(T)$ at low T. In fact, a clear change in slope and a crossover from a marginal-FL[8] to an insulating-like behavior above T^* is found, in good semiquantitative agreement with experiment[11–13] (see the inset). Simultaneously, the T dependence of in-plane resistivity [$\rho^{x,y}_{\rm dc}(T)$] (Refs. 11 and 12) is also consistent with data, apart from an overall overestimation: We obtain a good low-T metallicity and tendency towards a saturated behavior above 130 K, features characteristic of conventional (good) metals. Thus, our proposal provides a concrete link between ARPES and transport data, and is an attractive feature that goes beyond extant work. Further, the self-energies in Fig. 4 clearly show that m_z is heavily enhanced but $m_{x,y}$ remains light, also rationalizing the coexistent massless-Dirac and "heavy" carriers in graphite.[7] Finally, the small $E^*_F \simeq 20$ meV (Ref. 40) in graphite is also naturally understood: In graphite, the electron and hole pockets are a consequence of an interlayer hopping $t_\perp$ between p_z orbitals. In LDA, this is estimated to be 0.23 eV: Within the LDA, it would yield a much too large $E_F \simeq O(0.2)$ eV. However, in DMFT, the renormalized Fermi energy is $E^*_F = Z_{\rm FL} E_F \simeq 23$ meV, in accord with observations.[41]

Viewed in light of these results, our findings suggest interesting avenues for future study: (i) Can a multiband approach affirmatively resolve the issue of the g factor in graphite? (ii) Can suitable perturbations, e.g., intercalation, eliminate or enhance the low-T narrow Kondoesque peak and the associated tiny quasicoherent regime? This may be especially relevant for another longstanding issue of the *exotic* large positive magnetoresistance (MR)[5] and modest magnetic field-induced metal-insulator transition (MIT) in graphite. In our LDA + DMFT picture, a $O(1.0)$ T field will generically split the tiny "coherent" peak, and rapidly kill the tiny FL scale via a sizable spectral redistribution. Remarkably, since the peak is now related to three-dimensional (3D) FL coherence, its destruction will dynamically decouple neighboring layers, and the combination of reduced dimensionality and enhanced incoherence can readily give both large positive MR and a MIT, for example, via enhancement of excitonic tendencies by reduced itinerance.[42] On the other hand, certain rare-earth intercalants could further enhance SOC effects, stabilizing 3D FL-like coherence.[43] We will address these issues in future work.

III. CONCLUSION

In conclusion, based on a careful perusal of extant transport and PES data, we propose that, even with very wide p bands, sizable multiorbital electronic correlation-induced effective enhancement of the residual SOC plays a surprisingly essential role in resolving the enigma of the resistivity anisotropy, direction-selective incoherence-to-coherence crossover, and coexisting light and massive carriers in graphite. These turn out to be a manifestation of the incoherence-to-coherence crossover associated with a different version of the local Kondo effect, itself a consequence of an intricate interplay between Coulomb interactions and an *effectively* enhanced SOC in graphite. Our work provides a reliable microscopic template to further investigation of transport in graphite flakes[14] and multilayers, aspects which will be treated in future work. Finally, our microscopic description of coupled multiorbital interactions is expected to be generally applicable to partially filled p-band systems in general.[6,44]

ACKNOWLEDGMENTS

This work is supported by CAPES–Proc. No. 002/2012. Acknowledgment (A.S.A.) is also made to the FAPEMAT/CNPq (Project No. 685524/2010) for support. M.S.L. thanks T. Ziman for very helpful advice and ILL, Grenoble for financial support. S.L. is thankful to ZIH Dresden for computational time.

APPENDIX

Here we describe the procedure used to incorporate the spin-orbit coupling (SOC) in graphite into the DMFT calculations. Specifically, we will physically illustrate the mechanism which leads to an enhancement of the bare SOC, whose value in graphite is very small.

We start with the bare SOC Hamiltonian,

$$H_{\rm SOC} = \lambda \sum_i \mathbf{L}_i \cdot \mathbf{S}_i, \tag{A1}$$

which causes simultaneous spin and orbital flips. The bare λ is tiny in graphite, $O(1)$ K, and arises from the mixing between π and σ states by interlayer hopping $t_\perp$ (in LDA, $t_\perp \simeq 0.2$ eV $\gg \lambda$).[45] The bare value is thus too small to be of any relevance to the electronic structure of graphite. However, this bare SOC can get renormalized to effectively enhanced values if one explicitly considers electron correlations neglected in earlier work. We proceed as follows. Following Huber *et al.*,[23] we make the physically motivated approximation implied in the "rapid modulation limit" used there, and supported by electron-spin resonance (ESR) data. Our essential step is to notice that, in the multiorbital (MO) situation that is obtained in LDA + DMFT based approaches, the Hund's coupling $-J_H \sum_{i,a,b} \mathbf{S}_{i,a} \cdot \mathbf{S}_{i,b}$ gives rise to two main effects:

(i) When treated in DMFT, the static part of the self-energy now explicitly contains an extra term, apart from the normal Hartree term that is obtained in the absence of the SOC. Since, thanks to the approximation of Huber *et al.*,[23] we have $\langle a^\dagger_{i\uparrow} a_{i\downarrow}\rangle \neq 0$, the Hund term can now be "Hartree-Fock" (HF), factorized as

$$H_{\rm Hund} = -J_H \sum_{i,a,b} \mathbf{S}_{i,a} \cdot \mathbf{S}_{i,b} \longrightarrow \tag{A2}$$

$$H^{\rm MF}_{\rm Hund} = -J_H \sum_{i,a} \left[h_z S^z_{i,a} + h_- S^+_{i,a} + \text{H.c.}\right], \tag{A3}$$

where $h_z = \sum_b \langle S^z_{i,b}\rangle$ and $h_- = \sum_b \langle b^\dagger_{i,\downarrow} b_{i,\uparrow}\rangle$, etc. These effective fields renormalize the bare SOC couplings within the formalism used by Huber *et al.*, which we adopt.

(ii) This HF form in (i) is now used in the DMFT calculations along with the miniscule *bare* value of the SOC. Namely, we use the form

$$H_{\rm SOC} = \lambda \sum_{i,a,b} (\mathbf{L}_{i,a} - J_H \mathbf{S}_{i,b}) \cdot \mathbf{S}_{i,a}, \tag{A4}$$

along with Huber *et al.*'s approximation. In MO systems, anisotropic orbital-dependent renormalizations are generically known to lead to enhancement of bare atomic parameters, because the local correlation effects lead to a sizable reduction of the bare kinetic energy. As an example, it is known that strong correlation effects lead to drastic renormalization of the trigonal field in the classic Mott system V_2O_3.[46] It is natural to expect that correlation effects will also renormalize the bare SOC, apparent from the form of $H_{\rm SOC}$ above. Specifically, the "exchange fields" in $H^{\rm MF}_{\rm Hund}$ are enhanced by reduction of the LDA one-electron coherence as a result of correlation effects. From (i) above, we infer that it is J_H which will be the primary source of SOC enhancement by providing an "effective transverse field."[32] We have incorporated this effect in our calculation by starting with a term $V \sum_{i,a} (a^\dagger_{i,\uparrow} a_{i,\downarrow} + \text{H.c.})$ in the text, where V is taken to be a first estimate of the SOC (including bare and static HF contributions in the zeroth iteration of DMFT) that gets self-consistently renormalized further by DMFT due to generation of "internal fields" by Hund's coupling (see below).

(iii) Because the fermions in the three p orbitals have interband mixing matrix elements, having a finite (and now enhanced) SOC will generate renormalized interband spin-flip terms such as $t^{ab}_{\rm eff} \sum_{\langle i,j\rangle a,b} (a^\dagger_{i,\sigma} b_{j,-\sigma} + \text{H.c.})$ (these terms are already present in the *bare* $H_{\rm SOC}$,[45] but their magnitude is tiny), under renormalization. In DMFT, these terms act primarily to further modify the anisotropic renormalization of the MO spectrum. Specifically, since their physical nature is to cause additional transfer of dynamical spectral weight between different bands, this modifies orbital polarization and enhances orbital-selective coherence or incoherence. The specific effects on each band depend upon the details of the LDA DOS, and on the values of the local interaction parameters. In graphite, it turns out that the planar states are moderately affected, while those constituting the band dispersion along c are drastically renormalized as a consequence of this anisotropic renormalization. This is as it should be, since the interlayer states are much less dispersive than intraplane ones ($t_\perp \ll t_\parallel$ in LDA), and so are much more drastically affected by correlations.

Operationally, $\langle b^\dagger_{i,\downarrow} b_{i,\uparrow}\rangle$, for example, is computed from the off-diagonal Green's function $G^{\uparrow\downarrow}_{bb}(\omega) = \langle b_{i,\uparrow}; b^\dagger_{i,\downarrow}\rangle$

using the Lehmann representation, within the matrix-Green's function formulation in spin space. This is then substituted into $H^{\mathrm{MF}}_{\mathrm{Hund}}$ above, which thus appears as a renormalized effective "magnetic field" in the next DMFT iteration step,[32] and the process is iterated to convergence. The converged DMFT propagators are used to compute the in- and out-of-plane resistivities within the Kubo formulation, ignoring irreducible vertex corrections, which turn out to be small in the MO-DMFT formulation. The results are used in the main text.

Thus, J_H can enhance the effective SOC. This is similar to what has been proposed in an entirely different context of the spin-Hall effect,[47] where it is again MO correlations (specifically J_H) which are responsible for the enhancement of the effective SOC.

The approach outlined above may also permit an in-principle qualitative rationalization of a long-known problem: If the bare SOC in graphite is used to compute the g-factor anisotropy, the result, $\Delta g < 0$, is opposite to that found by ESR studies.[48] However, depending upon the extent of renormalization by MO correlations (specifically by J_H as above), the *effective* SOC will change sign if the bare SOC is extremely small and positive (as in graphite). Thus, if one now uses an effective SOC as above in graphite, $\Delta g > 0$ should result, in accord with ESR data. We have, however, not done this here.

[1] L. A., Nature (London) **105**, 372 (1920); R. W. Cahn and B. Harris, *ibid*. **221**, 132 (1969); F. Roberts, *ibid*. **198**, 420 (1963); R. Marom, S. F. Amalraj, N. Leifer, D. Jacob, and D. Aurbach, J. Mater. Chem. **21**, 9938 (2011).

[2] H. W. Kroto, J. R. Heath, S. C. O'Brien, R. F. Curl, and R. E. Smalley, Nature **318**, 162 (1985).

[3] S. Iijima, Nature (London) **354**, 56 (1991).

[4] K. S. Novoselov, D. Jiang, F. Schedin, T. J. Booth, V. V. Khotkevich, S. V. Morozov, and A. K. Geim, Proc. Natl. Acad. Sci. USA **102**, 10451 (2005).

[5] Y. Kopelevich, J. H. S. Torres, R. R. da Silva, F. Mrowka, H. Kempa, and P. Esquinazi, Phys. Rev. Lett. **90**, 156402 (2003).

[6] X. Du, S.-W. Tsai, D. L. Maslov, and A. F. Hebard, Phys. Rev. Lett. **94**, 166601 (2005).

[7] G. Li and E. Y. Andrei, Nat. Phys. **3**, 623 (2007).

[8] J. González, F. Guinea, and M. A. H. Vozmediano, Phys. Rev. B **59**, R2474 (1999).

[9] G. Baskaran and S. A. Jafari, Phys. Rev. Lett. **89**, 016402 (2002).

[10] K. S. Krishnan, Nature (London) **133**, 174 (1934).

[11] L. Edman, B. Sundqvist, E. McRae, and E. Litvin-Staszewska, Phys. Rev. B **57**, 6227 (1998).

[12] D. T. Morelli and C. Uher, Phys. Rev. B **30**, 1080 (1984).

[13] C. Uher, R. L. Hockey, and E. Ben-Jacob, Phys. Rev. B **35**, 4483 (1987).

[14] L. Casparis, D. Hug, D. Kölbl, and D. M. Zumbühl, arXiv:1301.2727.

[15] G. Moos, C. Gahl, R. Fasel, M. Wolf, and T. Hertel, Phys. Rev. Lett. **87**, 267402 (2001).

[16] J.-C. Charlier, X. Gonze, and J.-P. Michenaud, Phys. Rev. B **43**, 4579 (1991).

[17] J.-H. Wong, B.-R. Wu, and M.-F. Lin, Comput. Phys. Commun. **182**, 77 (2011).

[18] J. Mravlje, M. Aichhorn, T. Miyake, K. Haule, G. Kotliar, and A. Georges, Phys. Rev. Lett. **106**, 096401 (2011).

[19] A. Grüneis, C. Attaccalite, T. Pichler, V. Zabolotnyy, H. Shiozawa, S. L. Molodtsov, D. Inosov, A. Koitzsch, M. Knupfer, J. Schiessling, R. Follath, R. Weber, P. Rudolf, L. Wirtz, and A. Rubio, Phys. Rev. Lett. **100**, 037601 (2008).

[20] K. Sugawara, T. Sato, S. Souma, T. Takahashi, and H. Suematsu, Phys. Rev. B **73**, 045124 (2006).

[21] K. Sugawara, T. Sato, S. Souma, T. Takahashi, and H. Suematsu, Phys. Rev. Lett. **98**, 036801 (2007).

[22] L. Feng, X. Lin, L. Meng, J.-C. Nie, J. Ni, and L. He, Appl. Phys. Lett. **101**, 113113 (2012).

[23] D. L. Huber, R. R. Urbano, M. S. Sercheli, and C. Rettori, Phys. Rev. B **70**, 125417 (2004).

[24] G. Kotliar, S. Y. Savrasov, K. Haule, V. S. Oudovenko, O. Parcollet, and C. A. Marianetti, Rev. Mod. Phys. **78**, 865 (2006).

[25] L. Craco and S. Leoni, Phys. Rev. B **85**, 075114 (2012); **85**, 195124 (2012).

[26] G. Gui, J. Li, and J. Zhong, Phys. Rev. B **78**, 075435 (2008).

[27] O. K. Andersen, Phys. Rev. B **12**, 3060 (1975).

[28] R. Ahuja, S. Auluck, J. Trygg, J. M. Wills, O. Eriksson, and B. Johansson, Phys. Rev. B **51**, 4813 (1995).

[29] T. O. Wehling, E. Şaşıoğlu, C. Friedrich, A. I. Lichtenstein, M. I. Katsnelson, and S. Blügel, Phys. Rev. Lett. **106**, 236805 (2011).

[30] M. S. Dresselhaus, G. Dresselhaus, K. Sugihara, I. L. Spain, and H. A. Goldberg, in *Graphite Fibers and Filaments*, Springer Series in Materials Science (Springer, Berlin, 1988).

[31] G.-Y. Guo, S. Maekawa, and N. Nagaosa, Phys. Rev. Lett. **102**, 036401 (2009).

[32] L. Craco, J. Phys.: Condens. Matter **13**, 263 (2001).

[33] S. A. Jafari, Eur. Phys. J. B **68**, 537 (2009).

[34] J. A. Vergés, E. San Fabián, G. Chiappe, and E. Louis, Phys. Rev. B **81**, 085120 (2010).

[35] B. Reihl, J. K. Gimzewski, J. M. Nicholls, and E. Tosatti, Phys. Rev. B **33**, 5770 (1986).

[36] L. Craco, M. S. Laad, and E. Müller-Hartmann, Phys. Rev. B **74**, 064425 (2006).

[37] L. Craco, Phys. Rev. B **77**, 125122 (2008).

[38] N. S. Vidhyadhiraja, A. N. Tahvildar-Zadeh, M. Jarrell, and H. R. Krishnamurthy, Europhys. Lett. **49**, 459 (2000).

[39] J. Tomczak and S. Biermann, J. Phys.: Condens. Matter **21**, 064209 (2009).

[40] I. A. Luk'yanchuk and Y. Kopelevich, Phys. Rev. Lett. **93**, 166402 (2004).

[41] B. Fauqué, Z. Zhu, T. Murphy, and K. Behnia, Phys. Rev. Lett. **106**, 246405 (2011).

[42]D. V. Khveshchenko, Phys. Rev. Lett. **87**, 246802 (2001).
[43]T. E. Weller, M. Ellerby, S. S. Saxena, R. P. Smith, and N. T. Skipper, Nat. Phys. **1**, 39 (2005).
[44]D. Hsieh, D. Qian, L. Wray, Y. Xia, Y. S. Hor, R. J. Cava, and M. Z. Hasan, Nature (London) **452**, 970 (2008); F. Kuemmeth, S. Ilani, D. C. Ralph, and P. L. McEuen, *ibid*. **452**, 448 (2008).
[45]F. Guinea, New J. Phys. **12**, 083063 (2010).
[46]M. S. Laad, L. Craco, and E. Müller-Hartmann, Phys. Rev. Lett. **91**, 156402 (2003); A. I. Poteryaev, J. M. Tomczak, S. Biermann, A. Georges, A. I. Lichtenstein, A. N. Rubtsov, T. Saha-Dasgupta, and O. K. Andersen, Phys. Rev. B **76**, 085127 (2007).
[47]G. Y. Guo, S. Murakami, T.-W. Chen, and N. Nagaosa, Phys. Rev. Lett. **100**, 096401 (2008).
[48]M. Sercheli, Y. Kopelevich, R. R. da Silva, J. H. S. Torres, and C. Rettori, Physica B **320**, 413 (2002).